Macro Dark Matter

David M. Jacobs[1,2] **and Glenn D. Starkman**[1]

[1] *Center for Education and Research in Cosmology and Astrophysics*
Department of Physics and Institute for the Science of Origins,
Case Western Reserve University
[2] *Astrophysics, Cosmology and Gravity Centre*
Department of Mathematics and Applied Mathematics
University of Cape Town

E-mail: dm.jacobs@uct.ac.za, glenn.starkman@case.edu

Abstract: Dark matter is a vital component of the current best model of our universe, ΛCDM. There are leading candidates for what the dark matter could be (e.g. weakly-interacting massive particles, or axions), but no compelling observational or experimental evidence exists to support these particular candidates, nor any beyond-the-Standard-Model physics that might produce such candidates. This suggests that other dark matter candidates, including ones that might arise in the Standard Model, should receive increased attention. Here we consider a general class of dark matter candidates with characteristic masses and interaction cross-sections characterized in units of grams and cm^2, respectively – we therefore dub these macroscopic objects as *Macros*. Such dark matter candidates could potentially be assembled out of Standard Model particles (quarks and leptons) in the early universe. A combination of earth-based, astrophysical, and cosmological observations constrain a portion of the Macro parameter space; however a large region remains, most notably for nuclear-dense objects with masses in the range between about $50 - 10^{17}\mathrm{g}$ and $10^{20} - 10^{24}\mathrm{g}$.

Contents

1 Introduction

Observations on all scales from galaxies up indicate that, unless General Relativity (GR) requires serious modification, we live in a universe whose energy content is dominated by substances that differ from our everyday experience. The best dynamical model of the evolution of the Universe and its contents consistent with GR is ΛCDM, which describes a universe whose energy density is dominated on the largest scales by a cosmological constant ($\Omega_\Lambda \simeq 0.7$) and a non-relativistic matter component ($\Omega_m \simeq 0.3$). Observations of galaxies and clusters suggest that, assuming the correctness of Newton's inverse square law of gravity, they are heavily dominated by non-relativistic matter that cannot be accounted for in any census of their ordinary baryonic matter. At the same time, the observed primordial abundances of the light elements tell us that the fraction of the cosmological energy density that is due to baryons, $\Omega_b \lesssim 0.05 \ll \Omega_m$ [1, 2]. The remaining fraction of the non-relativistic matter, $\Omega_X \equiv \Omega_m - \Omega_b$, must be some kind of weakly-interacting matter that, apparently, is not a particle of the Standard Model.

The leading dark matter candidates are supersymmetric thermal relics, a class of stable weakly-interacting massive particles (WIMPs) that arise in certain theories of low-energy supersymmetry; however searches for supersymmetry at the LHC [3, 4] have so far failed to discover anything. Likewise, direct detection experiments [5–7] have yet to make any conclusive detection of conventional WIMPs.

We have few clues about the nature of the dark matter, except that, based on observations, it must satisfy a series of negative requirements: it shouldn't ruin the success of big bang nucleosynthesis (BBN) nor the physics of the cosmic microwave background (CMB); large scale structure must be allowed to grow to form galaxies and clusters, and the dark matter must remain undetected in any of the direct or indirection measurements. In fact, dark matter might only interact gravitationally – anything more than this would simply be the result of nature being kind to us. As usual, we proceed under this more optimistic assumption.

Let us take a step back to consider that there are two possibilities about the nature of the dark mater: (I) it is intrinsically weakly interacting, or (II) it is *effectively* weakly interacting because it is massive and hence has a much lower number density. Dark matter-baryon interaction rates go as $\sim n_{\rm X}\sigma_{\rm X}v$, the product of the dark matter number density, the interaction cross-section, and a characteristic velocity. Since $n_{\rm X} = \rho_{\rm X}/M_{\rm X}$ and $\rho_{\rm X}$ is fixed for any dark matter scenario, the event rate is proportional to $\sigma_{\rm X}/M_{\rm X}$, which we call the *reduced cross-section*. Conventionally, dark matter is dark because $\sigma_{\rm X}$ is small; this is possibility (I). But it can equally be dark if $M_{\rm X}$ is very large; this is case (II) and is what we are interested in this work. An interesting possibility that case (II) allows for is that the dark matter might still be accounted for within the Standard Model.

For example, given that the local dark matter density is measured to be about $7 \times 10^{-25}{\rm g/cm}^3$ [8] and the characteristic velocity of the dark matter is presumably about $10^{-3}c$, dark matter objects with masses on the order of $10^{18}g$ would hit the earth approximately once every billion years. At lower masses the frequency would be higher, but the nature of the impact matters greatly as to whether or not some signal is observable by

humans or if some historical record was left to be discovered.

Of course, this basic notion is not entirely new. Consider, for example, a proposal by Witten [9] wherein the QCD phase transition in the early universe resulted in an abundance of baryons alongside macroscopically sized/massed "nuggets" of quark matter with an approximate nuclear density of a few $\times\ 10^{14}\mathrm{g/cm}^3$. Estimates in that work suggested the mass of a typical nugget, which is posited to be the dark matter, could be $10^9 - 10^{18}$ g. At this range of masses, the expected rate of collision between such dark matter and the *entire* earth is at most once per year; clearly, underground detection experiments will have nothing to say about this possibility. Though the so-called WIMP miracle no longer applies, what is highly appealing in such a scenario is that little to no new physics is invoked to explain the origin of dark matter and, as a corollary, it offers a natural explanation as to why $\Omega_m \sim \Omega_b$.

There is an abundance of models directly (or indirectly) associated with this type of idea, for example: nuclearites [10], strangelets [11], strange baryon Q-Balls [12], baryonic colour superconductors [13, 14], compact composite objects (CCO's) [15], Compact Ultradense Objects (CUDOs) [16], and strange chiral liquids drops [17]. There are also primordial black holes (PBH) [18] and non-Standard Model models of such dark matter, such as Q-balls [19], and other objects not yet hypothesized that could make up some or all of the dark matter.

While specific theories have their own appeal, we find it prudent to try to understand the phenomenology of a general class of models in which the dark matter interacts with itself and normal matter strongly; in other words, its interaction probability is determined predominantly by geometry and kinematics. Existing constraints (as summarized in [20]) on strongly-interacting dark matter cover large regions of parameter space extending to masses of about 10^{17}GeV, prompting us to consider massive candidates with radius, R_{X} much larger than any microscopic length scale, e.g. the electron's Compton wavelength or the Bohr radius. We can then ignore any quantum-mechanical aspects of scattering, and any short-range interaction will simply be encoded in the dark matter's geometric[1] cross-section, $\sigma_{\mathrm{X}} = \pi R_{\mathrm{X}}^2$. It may also interact electromagnetically – we therefore consider dark matter objects with a charge Q_{X}. Generally, for these types of models the effective cross-section and mass are best quoted in cm^2 and g, respectively. We call this class of "macroscopic" dark matter *macro dark matter* and refer to the objects as *Macros*.

Assuming Macros are formed by some post-inflationary causal process, they have a maximum mass determined by the amount of dark matter within the causal horizon at the time of formation, $M_{H,\mathrm{dark}}$, given by

$$\begin{aligned} M_{H,\mathrm{dark}} &\simeq \frac{4\pi}{3}\rho_{\mathrm{X}}\left(T_\star\right) L_H^3 \\ &\sim 10^{35}\ \mathrm{g}\left(\frac{10^9\ \mathrm{K}}{T_\star}\right)^3 , \end{aligned} \tag{1.1}$$

[1] Gravitational focusing is negligible since the escape velocity is typically very small compared to the characteristic velocities of order $10^{-3}c$.

where $T_\star$ is the formation temperature. Although the dark matter could have formed as late as matter-radiation equality (if BBN is not disturbed), we shall assume the formation processes finished *before* the end of BBN occurred, i.e. $T_\star \gtrsim$ few$\times 10^9$K. Therefore in this work we consider only $M_{\rm X} \lesssim 2 \times 10^{34}{\rm g} = 10 M_\odot$.

The impact rate of an isotropic flux of Macros hitting a convex target object is[2]

$$\Gamma = \frac{1}{2} n_{\rm X} v_{\rm X} A_T f_G \,, \tag{1.2}$$

where A_T is the target area, $v_{\rm X}$ is the average Macro velocity, and $f_G = (1 + \frac{v_{\rm esc}^2}{v_{\rm X}^2})$ is the gravitational focusing factor. Altogether, the total impact rate is

$$\Gamma = 5.4 \times 10^5 \, {\rm s}^{-1} \left(\frac{1{\rm g}}{M_{\rm X}}\right) \frac{v_{\rm X}}{250 \text{ km/s}} \left(\frac{R_T}{R_\odot}\right)^2 \left(1 + 6.2 \frac{R_\odot}{R_T} \left(\frac{250 \text{ km/s}}{v_{\rm X}}\right)^2 \frac{M_T}{M_\odot}\right) f_\rho \,, \tag{1.3}$$

where M_T and R_T are the mass and radius of the target, $R_\odot = 7 \times 10^5$ km, $M_\odot = 2 \times 10^{33}$ g, we have used $M_{\rm X} n_{\rm X} = \rho_{\rm X} = 7.0 \times 10^{-25} {\rm g/cm}^3$ as the local dark matter density [8], and defined f_ρ as a density enhancement factor that is equal to unity in the solar neighborhood. In Table 1 we give the expected impact rates for various astrophysical objects.

Target	Γ $[M_{\rm X}^{-1}{\rm g\ s}^{-1}]$	Γ $[M_{\rm X}^{-1}{\rm g\ yr}^{-1}]$
NS	48	1.5×10^9
WD	4.8×10^3	1.5×10^{11}
$\odot$	3.9×10^6	1.2×10^{14}
$\oplus$	44	1.4×10^9
$\leftmoon$	3.2	1.0×10^8

Table 1. Expected Macro impact rates for a neutron star, white dwarf, the sun, the earth, and the moon. We have taken $v_{\rm X} = 250$ km/s, $R_{\rm NS} = 10$ km, $R_{\rm WD} = 10^3$km, $f_\rho = 1$, and $M_{\rm NS} = M_{\rm WD} = M_\odot$. For example, if $M_{\rm X} = 1$ g then there would be about 3 impacts per km^2 per year on the earth.

In Section 2 we give model-independent constraints, including those extant in or extracted from the published literature and applied to Macros. In Section 3 we give constraints that depend on specific Macro properties, such as electromagnetic charge. In Section 4 we report on considerations that do not appear to provide any useful constraints, and we make our concluding remarks in Section 5.

2 Model-Independent Constraints

2.1 Constraints at low masses

There are a variety of underground and space-borne detectors that have been used to put constraints on a large range of strongly-interaction dark matter parameters below 10^{17}GeV;

[2]The factor of 1/2 comes from the average of the component of the velocity vector normal to the surface, i.e. from the angular average of $\cos\theta$.

this is not the focus of the current work, but the list of model-independent constraints may be found in [20]. However, since the constraints obtained from the Skylab space station overlaps somewhat with our work here, we briefly summarize those results.

The Lexan (plastic) track detectors inside a wall of the Skylab space station [21] were used to probe the nature of cosmic rays and also were used to rule out a region of parameter space of strongly-interacting dark matter. The details of the dark matter constraints are discussed in Ref. [22] and we simply summarize the salient points below.

For elastically-scattering Macros, the energy loss rate of $\rho^{-1}dE/dx$ in the Lexan must have exceeded a minimum 400 MeV cm^2/g beyond which enough damage was done to the Lexan that an etchable track would have been seen. Since $\rho^{-1}dE/dx \simeq \sigma_{\rm X} v^2$, if $v_{\rm X} \simeq 250\,$km/s then the requirement is $\sigma_{\rm X} \geq 10^{-18}$ cm^2; this determines the bottom edge of the Skylab-constrained region of the $\sigma_{\rm X} - M_{\rm X}$ parameter space. The Macro also must penetrate a minimum distance of $x_{\rm min} \simeq 0.25$ cm while maintaining the above energy loss criterion for it to be visible. The velocity of such Macros will decrease in the material according to

$$v(x_{\rm min}) = v_0 e^{-\rho x_{\rm min}\sigma_{\rm X}/M_{\rm X}}\,. \tag{2.1}$$

As in [22], we assume $x_{\rm min} = 0.25$ cm so that $\rho x_{\rm min} \sim 0.25$ g/cm^2 which implies $\sigma_{\rm X}/M_{\rm X} \lesssim 3$ cm^2/g to use the Skylab constraints. For inelastically-scattering Macros, the requirement for an etchable track is that the hole cleared out in the Lexan could have been large enough that chemical reagents could have entered the hole during the etching process. This is plausible for hole radii larger than a few angstroms, or $\sigma_{\rm X} \gtrsim 10^{-15}$cm^2.

The total exposure of the Skylab experiment was on the order of 2 m^2 yr sr. Given a dark matter flux of $(4\pi)^{-1} n_{\rm X} v_{\rm X} \simeq 2\times 10^{17}({\rm GeV}/M_{\rm X})$ m^{-2} yr^{-1} sr^{-1}, the Skylab results rule out macro dark matter satisfying the above criteria for masses below about 10^{17}GeV $\simeq 2\times 10^{-7}$ g at greater than 95% confidence.

2.2 The Large-Scale Universe

2.2.1 CMB and Large-Scale Structure

In the standard collision-less dark matter scenario, the dark matter over-densities start to grow in earnest at the onset of matter domination at about $z \simeq 10^4$. Therefore, given the success of the CDM paradigm, we can get a sense of the kind of constraints obtainable by simply requiring that the DM has kinematically decoupled from baryons by this time. In a Macro-baryon collision the result of $M_{\rm X} \gg m_b$ on the kinematics indicates that the momentum imparted on a Macro, $\Delta p_{\rm X} \simeq m_b v_{\rm X}$. Therefore the average force on a Macro, given by the product of the baryon collision rate and the typical momentum transfer, is found to be

$$\begin{aligned}\langle F_{\rm X}\rangle &\simeq \Gamma_{{\rm X}b}\Delta p_{\rm X}\\ &\simeq \rho_b\sigma_{\rm X}\sqrt{\frac{T}{m_b}}v_{\rm X}\,.\end{aligned} \tag{2.2}$$

The relevant quantity is the ratio of this force to the Macro momentum, $M_{\rm X}v_{\rm X}$, which indicates the rate at which the kinematics of a Macro is significantly altered, and hence it

should be much less than the Hubble rate [23]. Therefore, requiring

$$\rho_b \frac{\sigma_{\rm X}}{M_{\rm X}} \sqrt{\frac{T}{m_b}} \ll H\,, \tag{2.3}$$

evaluated at $z_{\rm eq} = 10^4$, results in an expected constraint on the reduced cross-section

$$\frac{\sigma_{\rm X}}{M_{\rm X}} \ll 3 \text{ cm}^2/\text{g}\,. \tag{2.4}$$

Dark matter-baryon interactions would result in a drag force between the two fluids at early times and would act to dampen fluctuations [24]. The above approximation can be improved upon by several orders of magnitude by considering the detailed effects on the CMB and matter power spectra. In Ref. [25], the effects of velocity-dependent dark matter-baryon interactions on the CMB and Lyman-α power spectrum analysis were considered. To constrain Macro properties, we borrow those velocity-independent results to place a bound of

$$\frac{\sigma_{\rm X}}{M_{\rm X}} < 3.3 \times 10^{-3} \text{ cm}^2/\text{g} \tag{2.5}$$

at 95% confidence.

2.2.2 Heating and Cooling in Clusters

Virialized particles in a gravitational potential reach similar velocities; however when particles of different species collide there is there is a preferential energy transfer from massive to less massive particles, i.e. energy is transferred to drive the system toward thermal equilibrium. For this reason, Macros would provide a source of heat for gas in astrophysical systems, such as clusters. As was noticed by Chuznoy and Nusser [26] such gas heating, which would occur at a rate proportional to $\sigma_{\rm X}/M_{\rm X}$, can offset radiative cooling in the cores of clusters. To avoid conflict with observations, namely that gas temperatures do not increase toward the centers of clusters, they found an upper bound that corresponds to $\sigma_{\rm X}/M_{\rm X} < 10^{-25} cm^2/m_p = 0.06$ cm^2/g.

2.2.3 Self-Interacting Dark Matter

For a given dark-matter density ($\rho_{\rm X}$) and mean free path of $L_{\rm free}$ due to Macro-Macro collision the cross-section ($\sigma_{\rm XX}$) will obey the relation

$$\begin{aligned} \frac{\sigma_{\rm XX}}{M_{\rm X}} &= \frac{1}{\rho_{\rm X}} \frac{1}{L_{\rm free}} \\ &\simeq 0.5 \left(\frac{7.0 \times 10^{-25} \text{g/cm}^3}{\rho_{\rm X}} \right) \left(\frac{1 \text{ Mpc}}{L_{\rm free}} \right) \text{ cm}^2/\text{g}\,. \end{aligned} \tag{2.6}$$

Self-interacting dark matter was proposed to solve inconsistencies between CDM predictions and observations of structures on scales below a few Mpc, including the cusp-core and missing-satellite problems [27]. These inquiries have prompted several investigations of the strength of possible dark matter self-interactions. Simulations of galaxy cluster 1E 0657-56 (a.k.a. the bullet cluster) accounting for the self-interaction of dark matter result in

an offset between the bullet sub-cluster mass peak and galactic centroid; the absence of this observation in the actual cluster therefore provides a limit on $\sigma_{\rm X}/M_{\rm X}$ [28]. Comparisons were also made between simulations with self-interacting dark matter and the observed density profiles and substructure counts of other observed clusters, low-surface brightness spiral- and dwarf-spheroidal galaxies in Ref. [29]. Conservatively, both of the above constraints are approximately $\sigma_{\rm XX}/M \lesssim 1$ cm^2/g. From simple geometric considerations, the self-interaction cross-section of two Macro's is related to their geometric cross-section by a factor of 4, i.e. $\sigma_{\rm XX} = 4\,\sigma_{\rm X}$; therefore the constraints are $\sigma_{\rm X}/M_{\rm X} \lesssim 0.3$ cm^2/g for elastically-scattering Macros.

The constraint for inelastically-scattering Macros should be at least this strong, and comes from requiring that the Macros should have never collided on average. Requiring a mean free path greater than the distance traveled in the age of the universe, $v_{\rm X}\Delta t \simeq 10^{-3} c H_0^{-1} \simeq 3$ Mpc requires $\sigma_{\rm X}/M_{\rm X} \lesssim 0.04$. Stronger limits may still be obtainable on the inelastic case based on observations of dense galactic regions.

2.3 Ancient Mica

If the Macros have a low enough mass, their number density (and hence flux) would be high enough to have plausibly left a historical record on earth. If they have a low enough $\sigma_{\rm X}/M_{\rm X}$ so that they would have penetrated deep ($\sim$ a few km) into the earth's crust, a record would have been left in ancient muscovite mica. Searches for grand-unified-theory magnetic monopoles [30, 31] sought to detect lattice defects left in ancient mica, detectable through chemical etching techniques [32]. These same techniques were applied to put limits on the astrophysical flux of so-called nuclearites, in the range $10^{-16} - 10^{2}$g [10, 33]. Here we apply similar arguments to place constraints on a region of Macro parameter space.

The constraining power of mica is determined by a few factors. No significant detection was found in the sample in Ref. [31] which has an age of 500 Myr, a total area of 1200 cm^2, and was buried approximately 3 km underground. Using (1.2), an expected $\sim$ 165g of dark matter should have passed through the sample[3], or an average number of mica passages, $\lambda = 165{\rm g}/M_{\rm X}$. Since a Macro impact is a random (Poisson) process, the probability of n passages, $P(n)$, follows a Poisson distribution:

$$P(n) = \frac{\lambda^n}{n!} e^{-\lambda}\,. \tag{2.7}$$

Given the null observation, the value $\lambda \gtrsim 3$ may be ruled out at 95% confidence, or translating this to a bound on $M_{\rm X}$,

$$M_{\rm X} \lesssim 55\,{\rm g}\,, \tag{2.8}$$

where the mica constraints are applicable, however the bound is weakened to about 28 g for $\sigma_{\rm X} \gtrsim 10^{-8}\,{\rm cm}^2$. At a characteristic nuclear density of $3.6 \times 10^{14}\,{\rm g/cm}^3$, we infer

$$R_{\rm X} \gtrsim 3 \times 10^{-5}\ {\rm cm} \tag{2.9}$$

[3]This assumes that Macros pass undeterred straight through the earth. For $\sigma_{\rm X}/M_{\rm X} \gtrsim (\rho_\oplus R_\oplus)^{-1} \simeq 3 \times 10^{-10}$ cm^2/g the value of λ is decreased, and our Macro bound weakened, by a factor of 2.

if the Macro would admit a nuclear/QCD description.

There are also detection thresholds in velocity and energy deposition for elastic scattering. The Macro must have had a velocity greater than $2 \times 10^{-5} c$ upon reaching the buried mica[4]. For elastically-scattering Macros, the velocity at an average projected depth in the crust below the earth's surface, $\langle \rho L \rangle$, is approximately

$$v(L) = v_0 e^{-\langle \rho L \rangle \sigma_{\rm X}/M_{\rm X}} \,, \tag{2.10}$$

where we use $v_0 \equiv \langle v^2 \rangle^{1/2}$ as the initial velocity[5]. Taking $v_0 = 250 {\rm km}/s$ and $\langle \rho L \rangle = 10^6$ g/cm^2, the imposition of $v(L) > 2 \times 10^{-5} c$ requires

$$\frac{\sigma_{\rm X}}{M_{\rm X}} \lesssim 3.6 \times 10^{-6} \ {\rm cm}^2/{\rm g} \tag{2.11}$$

to obtain a constraint[6].

In order to have left an etchable track, there is also a minimum nuclear component of stopping power $S_n \equiv \rho^{-1} dE/dx \gtrsim 2.4$ GeV/g cm^2 [31]. For an elastically interacting Macro, $S_n \simeq \sigma_{\rm X} v\,(L)^2$, so constraints require

$$\sigma_{\rm X} \gtrsim 6 \times 10^{-18} \left(\frac{250 {\rm km}/s}{v(L)} \right)^2 \ \ [{\rm cm}^2] \,. \tag{2.12}$$

For masses above approximately 10^{-10}g we expect a track to have been left for $\sigma_{\rm X} \gtrsim 6 \times 10^{-18}$ cm^2. However at lower masses this inequality is less accurate since objects with smaller masses would have velocities that are more affected by their passage through the earth's crust.

For inelastic collisions, crustal material is accreted onto the Macro. Since our aim is to make a conservative, model-independent constraint we require that the Macro's velocity would have remained above a critical value, $v_c = \sqrt{\varepsilon/\rho} \simeq 0.2$ km/s, below which the energy loss from inter-molecular bond-breaking would have rapidly brought the Macro to rest; we have used a structural energy density of $\varepsilon \simeq 10^9$ erg/cm^3 as in [10]. For inelastic collisions, $v(L) = v_0 \left(1 + \langle \rho L \rangle \sigma_{\rm X}/M_{\rm X}\right)^{-1}$, therefore $v(L) > v_c$ implies $\sigma_{\rm X}/M_{\rm X} < v_0/v_c (\rho L)^{-1} \simeq 10^{-3}$ cm^2/g. The requirement for an etchable track is that the burrowed hole in the mica sample would have been large enough that hydrofluoric acid would have entered it during the etching process. This is plausible for hole radii larger than a few angstroms, so $\sigma_{\rm X} \gtrsim 10^{-15}$cm^2 should suffice. There could also be some charge-dependent enhancement to this process, however this is likely to be very material-dependent.

[4]This is due to kinematic reasons [30]; it corresponds to a nuclear energy transfer of about $0.2A$ eV, where A is the atomic number.

[5]Technically, the Macros would have velocities are drawn from a distribution, but the $\sigma_{\rm X}/M_{\rm X}$ requirement is only log-sensitive to the velocity, hence, we will ignore the tails of the distribution.

[6]In the crust $2.7 \lesssim \rho \lesssim 3.0\,{\rm g/cm}^3$. We conservatively use $\rho = 3\,{\rm g/cm}^3$ and a mica depth of $L = 3.5$ km to estimate $\langle \rho L \rangle$.

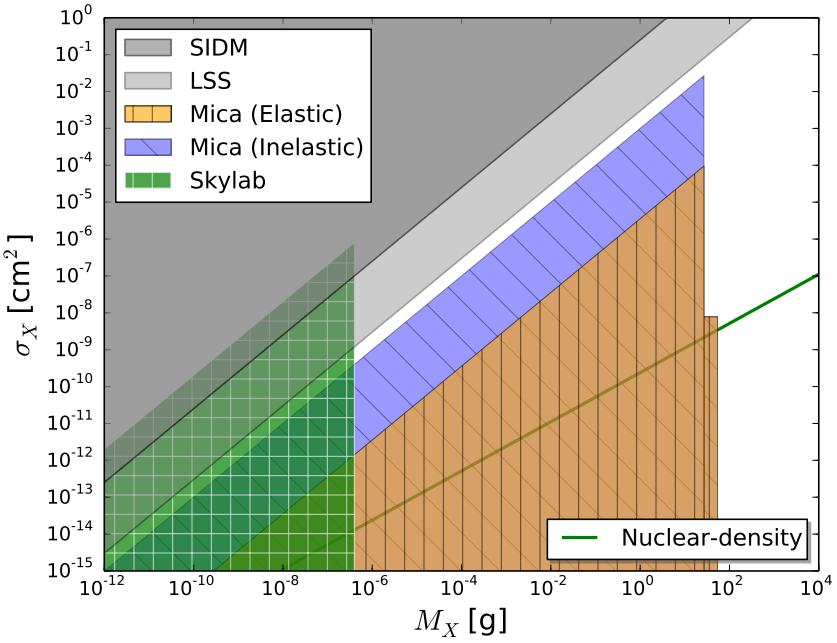

Figure 1. Macro constraints at low mass. In dark grey are those inferred from comparison of observed to numerically-simulated galaxies and clusters with self-interacting dark matter [28, 29]; overlapping, in light grey are the large-scale structure constraints borrowed from [25]; the orange and blue regions correspond to the mica constraints [31] on elastic- and inelastically-scattering Macros, respectively; the green region is the Skylab constraint [21, 22].

2.4 Gravitational Lensing

For an intervening mass between a light source and an observer, two images of the source can be observed, in principle. Below we give a brief review of the physics of lensing before proceeding to discuss how the phenomenon (or the lack of its observation) may be used to place constraints on the abundance of Macros.

We use the canonical variables to describe the the observer-lens and lens-source distances as $D_{\rm OL}$ and $D_{\rm LS}$, respectively. The total observer-source distance is the sum of the two, denoted $D_{\rm OS}$. Working in the lens plane with lens at the origin of coordinates, the line directly between the source and the observer is projected onto this plane at a distance, r_0, from the lens. Generally, the lens causes the observer to see two images[7]; the length scale characteristic of the impact parameter of a wave packet as it travels past the lensing mass is given by the Einstein radius,

$$R_E = \sqrt{4GM\frac{D_{\rm OL}D_{\rm LS}}{D_{\rm OS}}}\,. \tag{2.13}$$

Two electromagnetic waves passing in the vicinity of the lens with characteristic photon energy, E, and arriving at the location of the observer have amplitudes that add and

[7] If $r_0 \simeq 0$ then a so-called Einstein ring would be observed.

interfere, resulting in an intensity (or flux) amplification given by

$$A = \frac{2 + u^2 + 2\cos\Delta\phi}{u\sqrt{4+u^2}}\,, \tag{2.14}$$

where $u \equiv \frac{r_0}{R_E}$, and the phase difference $\Delta\phi = E\Delta r$ between the two waves is determined by both the energy of the photons and difference in their path lengths, Δr.

One way to detect the presence of an intervening lens is to look for a modulation of an observed photon flux as a function of E – this is the basic idea behind femtolensing [34]. When considering sources for which r_0 changes substantially in an observing time, the amplification would vary as a function of time – this is the basis of microlensing [35]. Historically, the above techniques have been used to place constraints on the abundance of primordial black holes, brown dwarfs, or other compact astrophysical objects comprising a fraction of the dark matter density. To constrain the abundance of Macros, we will (conservatively) insist that the Einstein lensing angle, $\theta_E = \sqrt{4GM_{\rm X}/d}$ exceed the angular size of the Macro, $\theta_X = R_{\rm X}/d$, for a characteristic distance, d. This amounts to the requirement

$$\sigma_{\rm X}/M_{\rm X} \lesssim 3 \times \left(\frac{d}{\rm Gpc}\right)\ {\rm cm}^2/{\rm g}\,. \tag{2.15}$$

2.4.1 Femtolensing

Femtolensing refers to gravitational lensing where the angular separation between two lensed images from the same source is of order 10^{-15} arcseconds. At such scales, images cannot be resolved, however an interference pattern in the energy spectrum of background sources would be observable. For a gamma-ray burst (GRB), for example, the magnification is energy-dependent and this results in an intensity pattern in the energy spectrum [34, 36].

The lensing probability is determined by the optical depth to the source, τ and a "lensing cross section" [36]. First, the optical depth may be calculated by noting that the cross section for "strong" lensing events is characteristically given by [37]

$$\begin{aligned}\sigma &= \pi R_E^2 \\ &= 4\pi G M_{\rm X} \frac{D_{\rm OL} D_{\rm LS}}{D_{\rm OS}}\,.\end{aligned} \tag{2.16}$$

The differential probability of a beam of light being a lensed by a cosmological distribution of Macros is then

$$\begin{aligned}d\tau &= n_{\rm X}\left(z_L\right)\sigma dt \\ &= \frac{3}{2}\Omega_{\rm X} H_0^2 \left(1+z_L\right)^3 \frac{D_{\rm OL} D_{\rm LS}}{D_{\rm OS}} \left(\frac{dt}{dz_L}\right) dz_L\,,\end{aligned} \tag{2.17}$$

where we have used $n_{\rm X}(z_L) = n_{\rm X}(0)\left(1+z_L\right)^3$, assumed the Macro population has not evolved significantly since z_L, used $n_{\rm X} = \rho_{\rm X}/M_{\rm X}$ and then invoked the Friedmann equation to write the fractional density of Macros as $\Omega_{\rm X}$. To the extent that the cross section is given by σ, this probability is therefore independent of $M_{\rm X}$.

For a light signal traveling past a massive source, the total geodesic distance from the source to the observer is given by [36]

$$\Delta\mathcal{D} \simeq \frac{1}{2}\frac{D_{\rm OS}}{D_{\rm LS}D_{\rm OL}}\left(r_-^2 - r_+^2\right) - 4MG\ln\frac{r_+}{r_-}\,, \tag{2.18}$$

where

$$r_\pm = \frac{1}{2}\left(r_0 \pm \sqrt{r_0^2 + 4R_E^2}\right)\,. \tag{2.19}$$

This is a *comoving* delay, however; in order to get the physical delay that accounts for cosmological expansion we note that the splitting of the image in time happens quite near the lens at redshift z_L, and so the physical delay is actually

$$\Delta r = (1+z_L)\Delta\mathcal{D}\,. \tag{2.20}$$

For a typical lens redshift of $z_L \simeq 1$, the period (in energy space) of the modulation signal is

$$\begin{aligned} E_p &= \frac{2\pi}{|\Delta r|} \\ &\sim \frac{10^{17}\text{g}}{M_{\rm X}}\ \text{MeV} \end{aligned} \tag{2.21}$$

This should be compared with both the energy range and resolution of the telescope used for the observation, since in order to see a fringe pattern in the source's spectrum it is required that a phase of ~ 1 be visible, therefore both $E_p \lesssim E_{ran}$ and $E_p \gtrsim E_{res}$ is required [36]. Given characteristic values of $E_{ran} = \mathcal{O}(1)$ MeV and $E_{res} = \mathcal{O}(1)$ keV for gamma-ray telescopes, constraints are possible in the range $10^{17} \lesssim M_{\rm X} \lesssim 10^{20}$ g.

Using this technique, the BATSE GRB data was used to rule out objects in the range $2\times10^{17} \lesssim M_{\rm X} \lesssim 2\times10^{20}$ g at 2σ from constituting a major fraction of the dark matter [38]. Recently, the GRB data taken by the Fermi satellite was used to rule out $10^{17} \sim 10^{19.5}$ g at 2σ [36]. The combined results allow us rule out Macros in the range $10^{17} \leq M_{\rm X} \leq 2\times10^{20}$. The sources and lenses are at a characteristic distance of $d \sim$ Gpc, so equation (2.15) allows us to apply this constraint for $\sigma_{\rm X}/M_{\rm X} \lesssim 1$ cm^2/g. Lastly, we note that in Ref. [39] it is claimed that the constraints in Ref. [36] were obtained ignoring finite-source effects, so it is with this caution that we employ their results.

2.4.2 Microlensing

Microlensing of a background light source by an intermediate gravitationally-lensing object results in a short-term change in the observed brightness of the source as the lens passes near the line of sight. In order for the microlensing of a source to be seen, it should lie approximately inside the Einstein ring of the lens, setting a minimum size of the ring at some characteristic distance. Taking a characteristic angle given by $\theta_E \approx \sqrt{4GM_{\rm X}/D_{\rm OS}}$ and a characteristic source radius of one solar radius ($R_\odot = 7\times10^5$km), one requires

$$\sqrt{\frac{4GM_{\rm X}}{D_{\rm OS}}} \gtrsim \frac{R_\odot}{D_{\rm OS}}$$

or

$$M_{\rm X} \gtrsim 10^{-7} M_\odot \,,$$

where we've used the distance to the Large Magellanic Cloud of about 50 kpc $\simeq 1.5 \times 10^{18}$ km as a fiducial value for $D_{\rm OS}$. The transit time for an object to pass through the corresponding Einstein radius is roughly

$$\begin{aligned} \Delta t &= \frac{2R_E}{v_{\rm X}} \\ &\simeq 10^7 \text{ s} \sqrt{\frac{M_{\rm X}}{M_\odot}} \,, \end{aligned} \tag{2.22}$$

which sets the range of possible constraints due to finite observing times. For example, a Macro of mass $M_{\rm X} = 10^{-7} M_\odot = 2 \times 10^{26}$ g would take about an hour to make the transit while $M_{\rm X} = 10\, M_\odot = 2 \times 10^{34}$ g would take about a year, assuming the source is in the Large Magellanic Cloud.

Constraints were put on such massive objects through the monitoring of sources in the Small and Large Magellanic Clouds, ruling out dark matter candidates in the range $1.2 \times 10^{26} - 6 \times 10^{34}$ g [40–42]. Given characteristic distances of about 50 kpc, equation (2.15) tells us we can apply that constraint when $\sigma_{\rm X}/M_{\rm X} \lesssim 10^{-4}$ cm^2/g. In Ref. [43], observations provided by the Kepler satellite were similarly used to make constraints on the range $4 \times 10^{24} - 2 \times 10^{26}$ g. At typical distances of about 1 kpc, equation (2.15) indicates these limits are applicable for $\sigma_{\rm X}/M_{\rm X} \lesssim 10^{-6}$ cm^2/g. A summary of constraints are illustrated in Figure 2.

3 Model-Dependent Constraints

3.1 Electromagnetic Properties of Models I, II, and III

There is an inherent difficulty in making predictions about the way macro dark matter would behave electromagnetically without knowing its precise composition, even if it is Standard Model in origin. Different models exist in the literature that predict wildly different properties, primarily owing to whether or not electrons (positrons) can penetrate into them. We can separate the nuclear-inspired Macro models into three broad classes:

- I) The net core charge, $Q_{\rm X} = 0$
- II) There is a non-trivial $Q_{\rm X} - R_{\rm X}$ relationship, but the Macros do not admit $e^\pm$
- III) Same as II), but the Macros do admit $e^\pm$.

For model types II) & III) we will assume the $Q_{\rm X} - R_{\rm X}$ relationship is maintained by the requirement that the surface potential owing to the core (quark) charge remains constant, i.e.

$$V_0 = \frac{Q_{\rm X}\alpha}{R_{\rm X}} \,, \tag{3.1}$$

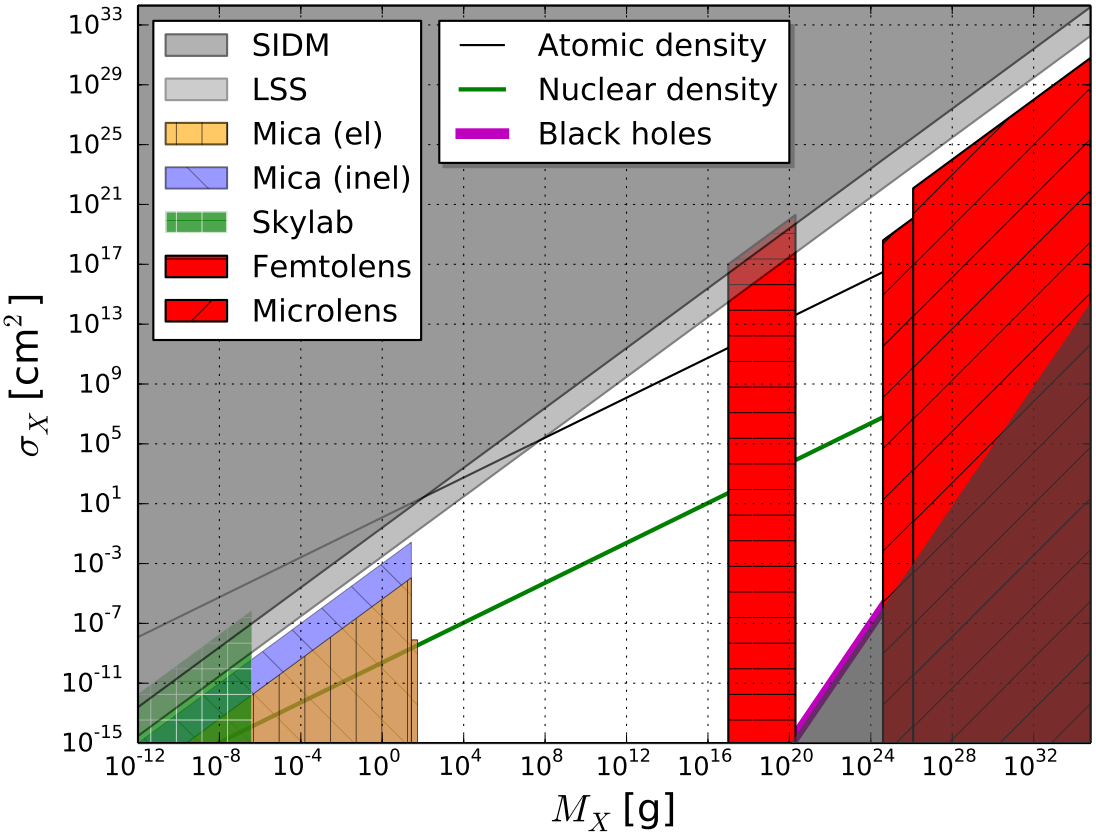

Figure 2. Summary of model-independent constraints. Compared to Figure 1, we have added in red the femto- and micro-lensing constraints taken from [36, 38, 40–43]. The black and green lines correspond to objects of constant density 1 g/cm^3 and 3.6×10^{14} g/cm^3, respectively. Viable black hole candidates lie on the magenta line; objects within the shaded region in the bottom-right corner should not exist as they would simply be black holes.

where V_0 is fixed, implying

$$|Q_{\rm X}| \simeq 1.1 \times 10^5 \left(\frac{|V_0|}{15\ {\rm MeV}}\right)\left(\frac{R_{\rm X}}{10^{-8}{\rm cm}}\right) . \tag{3.2}$$

Model II makes for very tractable calculations, since the surface potential is fixed at a constant value, however model III requires additional statistical-mechanical considerations.

3.1.1 Model III

Since a detailed description of the core charge distribution within the Macro is unknown, we take it to be uniform. In the places/eras of interest, the Macros will be immersed in a fluid of protons, electrons and, depending on the era, positrons. We will assume the overall distribution of the fluid to be determined by the hydrostatic equilibrium between the fluid pressure and the electrostatic force.

Recall that the number densities and pressures of a fermion species are given by

$$n_i = \frac{1}{\pi^2}\int_{m_i}^{\infty} d\widetilde{E}\,\frac{\widetilde{E}\sqrt{\widetilde{E}^2 - m_i^2}}{e^{(\widetilde{E}+V_i-\mu_i)/T}+1} \tag{3.3}$$

$$P_i = \frac{1}{3\pi^2}\int_{m_i}^{\infty} d\widetilde{E}\,\frac{\left(\widetilde{E}^2 - m_i^2\right)^{3/2}}{e^{(\widetilde{E}+V_i-\mu_i)/T}+1}\,, \tag{3.4}$$

where here $\widetilde{E}$ is only the relativistic part of the energy, i.e. $E = \widetilde{E} + V_i$, where E is the full energy eigenvalue of the Hamiltonian. Using this definition, the chemical potentials, μ_i are the same as their background values in the absence of the Macro. In the classical limit, applicable in the cases of interest, the exponential dominates in the denominators and one finds

$$n_i = e^{-V_i/T}\bar{n}_i \tag{3.5}$$

$$P_i = e^{-V_i/T}\bar{n}_i T\,, \tag{3.6}$$

where the barred values are the background values, and we have defined $V_{e^-} \equiv V$ so that $V_{e^+} = V_p = -V$.

Since the system is taken to be spherically symmetric, the condition for electric hydrostatic equilibrium is

$$\frac{dP}{dr} = \frac{Q_{\rm int}(r)\alpha}{r^2}\left(-n_{e^-} + n_{e^+} + n_p\right)\,, \tag{3.7}$$

where $Q_{\rm int}\,(r)$ is the (integer) charge within a sphere of radius, r, and is given by

$$Q_{\rm int}\,(r) = \begin{cases} Q_{\rm X}\left(\dfrac{r}{R_{\rm X}}\right)^3 + 4\pi\displaystyle\int_0^r d\widetilde{r}\;\widetilde{r}^2\,(n_p + n_{e^+} - n_{e^-}) & (r < R_{\rm X}) \\ Q_{\rm X} + 4\pi\displaystyle\int_0^r d\widetilde{r}\;\widetilde{r}^2\,(n_p + n_{e^+} - n_{e^-}) & (r > R_{\rm X})\,. \end{cases} \tag{3.8}$$

In the limit $r \to 0$, one can show that $dP/dr \to 0$ for a reasonably well-behaved potential[8], indicating

$$V'(0) = 0\,. \tag{3.9}$$

The other boundary condition on V comes from the requirement

$$\lim_{r\to\infty} V(r) \to 0 \tag{3.10}$$

The value of $V(0)$ will generally not be known, except for when a full analytic solution for $V(r)$ is available, hence numerical "shooting" will be required in order to numerically evolve $V(r)$ from $r = 0$. The differential equation to solve is found by taking a derivate of (3.7) with respect to r, which simply results in a version of the Poisson equation[9]

$$V''(r) + \frac{2}{r}V'(r) = 4\pi\alpha\Big(\pm\, n\,\Theta(R_{\rm X} - r) + n_p + n_{e^+} - n_{e^-}\Big)\,, \tag{3.11}$$

[8] This is true if $V(r)$ is finite at $r = 0$, for example.

[9] This is consistent with our convention that $V = -e\phi$, where ϕ is the electrostatic potential; it satisfies $\nabla^2\phi = -\rho$, where ρ is the charge density.

where $n \equiv 3\,|Q_{\rm X}|\,/(4\pi R_{\rm X}^3)$, and upper or lower signs refer to $Q_{\rm X} > 0$ or $Q_{\rm X} < 0$, respectively. After dividing by T, defining $q^2 \equiv 4\pi\alpha n/T$, $y \equiv qr$, and $v(y) \equiv V/T$, we arrive at the dimensionless equation

$$\ddot{v}(y) + \frac{2}{y}\dot{v}(y) = \pm\Theta\left(y_{\rm X} - y\right) + \frac{n_p + n_{e^+} - n_{e^-}}{n}\,, \tag{3.12}$$

where a dot is a derivative with respect to y and $y_{\rm X} \equiv qR_{\rm X}$. Generally, this equation must be solved numerically; however, in the case $|v(y)| \ll 1$ it is easy to show that

$$n_p + n_{e^+} - n_{e^-} \simeq \left(\bar{n}_p + \bar{n}_{e^+} + \bar{n}_{e^-}\right) v(y) \tag{3.13}$$

due to overall charge neutrality. Therefore the solution to (3.12) is approximately

$$v(y) = \begin{cases} \mp\left(\dfrac{1}{a^2} - c_1\dfrac{e^{ay} - e^{-ay}}{y}\right) & (y < y_{\rm X}) \\ \pm c_2\dfrac{e^{-ay}}{y} & (y > y_{\rm X})\,, \end{cases} \tag{3.14}$$

where $a^2 \equiv \bar{n}/n$ and $\bar{n} \equiv \bar{n}_p + \bar{n}_{e^+} + \bar{n}_{e^-}$. By the matching of $v(y_{\rm X})$ and $\dot{v}(y_{\rm X})$ at $y_{\rm X}$ we learn

$$c_1 = \frac{1}{2a^3}e^{-ay_{\rm X}}\left(1 + ay_{\rm X}\right) \tag{3.15}$$

$$c_2 = \frac{1}{a^3}\left(\sinh ay_{\rm X} - ay_{\rm X}\cosh ay_{\rm X}\right)\,. \tag{3.16}$$

In order to use these solutions, we must establish their range of validity. Given that $|v(y)|$ is known to decrease monotonically with increasing y, these solutions will be appropriate if $|v(0)| \ll 1$ and so we would like to know for what $Q_{\rm X} - R_{\rm X}$ relation this is true. It is therefore checked in two limits:

- $ay_{\rm X} \ll 1$: Here $|v(0)| \simeq y_{\rm X}^2/2$, from which it is required that

$$|Q_{\rm X}| \ll \frac{2}{3}\frac{R_{\rm X}T}{\alpha}\,. \tag{3.17}$$

- $ay_{\rm X} \gg 1$: Here $|v(0)| \simeq n/\bar{n}$, and therefore it is required that

$$|Q_{\rm X}| \ll \frac{4\pi}{3}R_{\rm X}^3\bar{n}\,. \tag{3.18}$$

Given the above results, we consider two two eras/systems that are of interest: BBN and stellar cores.

BBN ($T = 1$ MeV): Here $\bar{n} \simeq 5 \times 10^{31}{\rm cm}^{-3}$, therefore $ay_{\rm X} \simeq \frac{R_{\rm X}}{10^{-10}{\rm cm}}$. The mica limit (2.9) indicated that such nuclear-dense Macros are only possible for $R_{\rm X} \gtrsim 3 \times 10^{-5}$ cm, and therefore the small $|v|$ is guaranteed if (3.18) is satisfied. Given the $Q_{\rm X} - R_{\rm X}$ relationship of (3.2), this requires

$$R_{\rm X} \gg 2 \times 10^{-10}\sqrt{\left|\frac{V_0}{15\ {\rm MeV}}\right|}\ \ [\,{\rm cm}\,]\,, \tag{3.19}$$

which is easily satisfied in nuclear-inspired models where $|V_0| \sim \mathcal{O}(10)$ MeV (see e.g. [44–46]) [10].

Stellar Core ($T \simeq 1$ keV): Here we take the solar value of $\bar{n} = n_{\odot,\rm core} \simeq 2 \times 10^{26} {\rm cm}^{-3}$, therefore $a y_{\rm X} \simeq \frac{R_{\rm X}}{2\times 10^{-9}{\rm cm}}$. Again, the mica limit indicates that small $|v|$ is guaranteed if (3.18) is satisfied. Given the nuclear model of (3.2), this requires

$$R_{\rm X} \gg 10^{-7} \sqrt{\left| \frac{V_0}{15 \text{ MeV}} \right|} \ [\,{\rm cm}\,], \tag{3.20}$$

which is also easily satisfied in the representative models mentioned above. In summary, we have established that $V(0) < T$, and hence $V(R_{\rm X}) < T$ in both of the above systems, indicating that there is no significant Coulomb barrier to prevent protons from entering the Marcos of model III during BBN or inside a typical stellar core today.

3.2 BBN Limits on Model II

A Macro could affect the path of standard model particles, possibly absorbing them or even catalyzing their decay, as in the scenario of supersymmetric Q-balls [47]. If Macros absorbed a significant fraction of the ambient neutrons and a negligible fraction of protons, for example, the standard BBN predictions would be altered; this was noted, for example, in the context of strange nuclear matter [48]. Since nearly all surviving neutrons during BBN end up in ^{4}He, the primordial helium mass fraction, X_4 is

$$X_4 = \frac{2 n_n}{n_n + n_p}, \tag{3.21}$$

which has been measured at the few percent level using observations of metal-poor extragalactic H II regions [49]. A modest decrement in the relative abundance of neutron or protons would then significantly affect this observable quantity. Model types I and III would allow protons into the Macro at nearly the same rate as neutrons, so an effect on the primordial abundances of the light elements is not expected[11]. *The following constraints therefore only apply to model type II.*

Before comparing to theory one must be careful, however, as this effect is degenerate with other possibilities that could affect the measured value of X_4, such as the existence of extra relativistic species (ΔN_ν) or errors in the measurement of the baryon fraction (Ω_b),

[10] Although BBN occurs between temperatures of about 1 MeV to 0.1 MeV, it is during the higher temperature (earlier time) era that the majority of nucleon absorption would occur and have a possible effect.

[11] Of course, this is true unless the Macros were to have swept up a large fraction of the total number of baryons, and this depends on $\sigma_{\rm X}/M_{\rm X}$ and the Macro formation temperature. We would worry if

$$\frac{\Delta M_{\rm X}}{M_{\rm X}} \sim 10^6 \frac{\sigma_{\rm X}}{{\rm cm}^2} \frac{1\ {\rm g}}{M_{\rm X}} T_{9,form}^{3/2} \sim \mathcal{O}(1)\,.$$

If the formation temperature was 150 MeV, for example, then $T_{9,form} \simeq 2 \times 10^3$ and we would require $\sigma_{\rm X}/M_{\rm X} \ll 10^{-10}$ cm^2/g to ensure $\frac{\Delta M_{\rm X}}{M_{\rm X}} \ll 1$, thereby guaranteeing that most of the baryons were not swept up by the Macros. This would require $M_{\rm X} \gg 1$g, which is marginally satisfied by the mica constraints.

loosening any constraint to some degree; the current experimental error bars in e.g. Ref. [49] are still large enough to justify neglecting this degeneracy, however. The results from that work indicate that the observed abundance $X_4^{\rm obs} \simeq 0.25 \pm 0.01$, while the standard theoretical prediction, $X_4^{\rm std} = 0.2485 \pm 0.0002$. Therefore if we characterize a deviation due to Macros by

$$X_4 = X_4^{\rm std} + \Delta X_4^{\rm Macro} \tag{3.22}$$

we conclude the observational bound

$$-0.01 \lesssim \Delta X_4^{\rm Macro} \lesssim 0.01 \tag{3.23}$$

since the uncertainty on $X_4^{\rm std}$ is negligible.

To calculate $\Delta X_4^{\rm Macro}$, we use the comoving proton and neutron number densities

$$\mathcal{N}_{n,p} \equiv a(t)^3 \; n_{n,p} \,, \tag{3.24}$$

where $a(t)$ is the cosmological scale factor. For the accuracy required here it suffices to use the approximate evolution equations

$$\dot{\mathcal{N}_n} = -\left(\Gamma_n + \Gamma_{nX}\right) \mathcal{N}_n \tag{3.25}$$

$$\dot{\mathcal{N}_p} = +\Gamma_n \mathcal{N}_n - \Gamma_{pX} \mathcal{N}_p \,. \tag{3.26}$$

Here Γ_n is the neutron decay rate, and Γ_{nX} (Γ_{pX}) is the rate of neutron (proton) absorption[12] by Macro. Most relevant for computing the effects on the ^{4}He abundance is the proton to neutron ratio

$$\alpha(t) \equiv \frac{n_p}{n_n} = \frac{\mathcal{N}_p}{\mathcal{N}_n} \,, \tag{3.27}$$

from which we may write

$$X_4(t) = \frac{2}{\alpha(t) + 1} \,. \tag{3.28}$$

From (3.25) and (3.26), $\alpha(t)$ obeys the evolution equation

$$\dot{\alpha}(t) = \Gamma_n + \left(\Gamma_n + \Gamma_X\right) \alpha(t) \,, \tag{3.29}$$

where $\Gamma_X \equiv \Gamma_{nX} - \Gamma_{pX}$. The solution is

$$\alpha\left(t\right) = \left(\alpha_0 + \int_{t_0}^{t} d\tilde{t} \; \Gamma_n e^{-\int_{t_0}^{\tilde{t}} dt' \; \left(\Gamma_n + \Gamma_X\right)}\right) e^{\int_{t_0}^{t} dt'' \; \left(\Gamma_n + \Gamma_X\right)} \,, \tag{3.30}$$

where α_0 is set by the proton-to-neutron ratio at the time of weak-interaction freeze-out, which we presume to be unaffected by the presence of Macros. Technically, Γ_n is temperature dependent [50, 51] but it was found that including this effect only changes our results by roughly 0.1%. The Macros' effect would apparently be small, so we expand in $\int \Gamma_X$, finding

$$\alpha(t_B) = \alpha^{\rm std}(t_B) \left(1 + a\right) - b, \tag{3.31}$$

[12] This is also appropriate if the Macro catalyzes the baryon to decay to something non-baryonic.

where $\alpha^{\rm std}(t_B)$ is the standard value and

$$a = \int_{t_F}^{t_B} dt\ \Gamma_X \tag{3.32}$$

$$b = e^{\int_{t_F}^{t_B} dt\ \Gamma_n} \int_{t_F}^{t_B} d\tilde{t}\ \Gamma_n\ e^{-\int_{t_F}^{\tilde{t}} dt\ \Gamma_n} \int_{t_F}^{\tilde{t}} dt\ \Gamma_X\,. \tag{3.33}$$

We denote t_F as the time of weak-interaction freeze-out and t_B as the time of the deuterium bottleneck breaking; to good approximation, this defines the time of efficient ^{4}He production – thus X_4 is largely determined by $\alpha(t_B)$. Given that $X^{\rm std} \simeq 0.25$ (or $\alpha^{\rm std}(t_B) \simeq 7$), we find

$$\Delta X_4^{\rm Macro} \simeq -\frac{7a-b}{32}\,. \tag{3.34}$$

To perform the integrals in a and b, we change our integration variable to temperature using the time-temperature relation

$$t = \frac{\theta}{T_9^2}\ [\,s\,]\,, \tag{3.35}$$

where T_9 is the temperature defined in units of 10^9K and θ depends on the number of relativistic degrees of freedom. As in [52], we find

$$\theta = \begin{cases} 99.4, & T_9 > 5 \\ 178, & T_9 < 1\,, \end{cases} \tag{3.36}$$

assuming the standard value of $N_{\rm eff} = 3.046$. In what follows, we use the values[13] $T_{9,F} = 9.1$ and $T_{9,B} = 1$ and numerically determine a and b for different Macro properties. Integrating through this range requires an interpolation of $\theta(T_9)$ in the region $1 \le T_9 \le 5$; to do this we choose a hyperbolic tangent centered around $T_9 = 2$:

$$\theta(T_9) \simeq \theta_{\rm max} - \frac{1}{2}\left(\theta_{\rm max} - \theta_{\rm min}\right)\left(\tanh\left[T_9 - 2\right] + 1\right)\,, \tag{3.37}$$

where $\theta_{\rm max} = 178, \theta_{\rm min} = 99.4$. The general formula (3.37) is sufficient to match all of the values quoted in Table 15.5 of Ref. [53] to an error of less than 10%, which is sufficient for our purposes[14].

Since a neutron is neutral, its absorption rate by Macros is given by

$$\Gamma_{nX} = \langle \frac{\rho_{\rm X}}{M_{\rm X}} \sigma_{\rm X} v \rangle \tag{3.38}$$

$$= 5.1 \times 10^4 \times T_9^{7/2} \frac{\sigma_{\rm X}}{M_{\rm X}} \frac{\rm g}{\rm cm^2\ s}\,, \tag{3.39}$$

where we have used the thermally-averaged neutron velocity $v_n = \sqrt{8T/(\pi m_n)}$ and inserted $\rho_{\rm X} = 3H_0^2/(8\pi G)\Omega_c\,(T/T_0)^3 = 0.93 \times 10^{-3}\Omega_c h^2 T_9^3$ g/cm^3 with the Planck value of $\Omega_c h^2 = 0.1199$ [2].

[13] These were the values used in [52]. Changing them by 10% affects the integrals only at the few-percent level.

[14] Ref. [53] used two neutrino species to calculate Table 15.5 therein; to compare to it, $\theta_{\rm max}$ and $\theta_{\rm min}$ must be corrected to account for this smaller number of relativistic fermions.

For a proton of energy E_p incident on a Macro with surface potential $V(R_{\rm X})$ the effective cross-section, $\sigma_{\rm X,eff} = \sigma_{\rm X}\left(1 - \frac{V(R_{\rm X})}{E_p}\right)$. This must be thermally averaged along with the velocity, resulting in

$$\langle \sigma_{\rm X,eff} v \rangle = \sigma_{\rm X} \times \begin{cases} e^{-\frac{V(R_{\rm X})}{T}} \langle v \rangle, & V(R_{\rm X}) \geq 0 \\ \left(1 - \dfrac{V(R_{\rm X})}{T}\right) \langle v \rangle, & V(R_{\rm X}) < 0\,. \end{cases} \tag{3.40}$$

It then follows that the proton absorption rate may written in terms of the neutron rate as

$$\Gamma_{pX} = \Gamma_{nX} \times \begin{cases} e^{-V(R_{\rm X})/T}, & V(R_{\rm X}) \geq 0 \\ \left(1 - \dfrac{V(R_{\rm X})}{T}\right), & V(R_{\rm X}) < 0\,. \end{cases} \tag{3.41}$$

For positive surface potentials there is a Boltzmann-Coulomb suppression for the absorption rate, whereas if it is negative there is a Coulomb enhancement. We do not allow $V(R_{\rm X})$ to evolve, in accordance with nuclear model II.

Combining the predicted Macro effect of $\Delta X_4^{\rm Macro}$ (3.34) and the observational bound (3.23), we find that

$$\frac{\sigma_{\rm X}}{M_{\rm X}} \lesssim 8 \times 10^{-11} \left| \frac{V(R_{\rm X})}{\rm MeV} \right|^{-1} \ {\rm cm}^2/{\rm g}\,, \tag{3.42}$$

for $V(R_{\rm X}) \lesssim 0.01$ MeV, while for $V(R_{\rm X}) \gtrsim 1$ MeV we find the bound asymptotes to

$$\frac{\sigma_{\rm X}}{M_{\rm X}} \lesssim 2 \times 10^{-10} \ {\rm cm}^2/{\rm g}\,. \tag{3.43}$$

In between there is a transition, illustrated in Figure 3.

As an example, for nuclear-type models with $V(R_{\rm X}) \simeq -20$ MeV as suggested in e.g. [44–46], the constraint would be $\sigma/M_{\rm X} \lesssim 4 \times 10^{-12}$ cm^2/g if such Macros absorb protons. At nuclear density ($\simeq 3.6 \times 10^{14}$g/cm^3) this translates to a bound on the mass of $M_{\rm X} \gtrsim 3 \times 10^5$ g, an improvement over the limit from ancient mica by nearly 4 orders of magnitude.

3.3 "Converting" Dark Matter

Should the dark matter be of some more stable form of matter than ordinary baryons, it is conceivable that it could convert astrophysical objects to its form; this is thought to occur in various models of stable strange matter, where normal baryonic matter is converted to this state (see e.g. [9], [44]). If the dark matter were of this type of "converting" variety, it could potentially convert any target that it gets captured inside of, such as the sun or a neutron star, for example. This is necessarily model dependent – in model II, for example, the Macro cannot easily absorb protons when $V_0 \gg 1$ keV and so it would be incapable of converting a typical star. On the other hand, a neutron star can be used, in principle, for constraints in a more model-independent way since the absorption of neutrons is independent of the Macro charge.

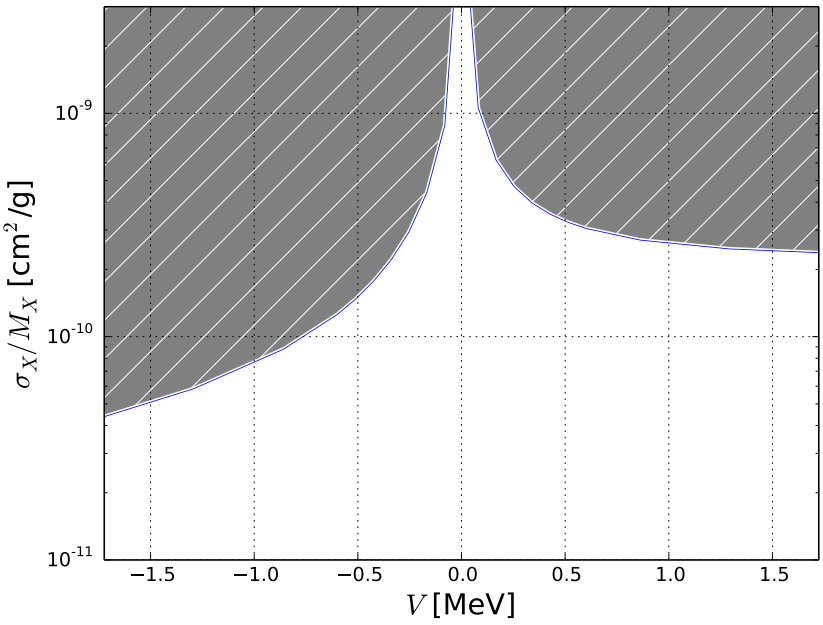

Figure 3. Model-dependent constraints from BBN on $\sigma_{\rm X}/M_{\rm X}$ as a function of the Macro surface potential, in model II. The parameter space ruled out lies in the grey region.

For a Macro of mass $M_{\rm X}$ passing through an astrophysical spherical target on a secant line of length, D, it can be shown that its velocity in the target evolves according to

$$\frac{dv}{dx} = -\rho_T \frac{\sigma_{\rm X}}{M_{\rm X}(x)} v(x) + \frac{4\pi}{3} \frac{G\rho_T \left(\frac{D}{2} - x\right)}{v(x)}\,, \tag{3.44}$$

where ρ_T is the average target density. $M_{\rm X}(x)$ is constant for elastically-scattering Macros and is a linear function of x, the passage depth, in the inelastic case. We define the dimensionless parameter $\alpha \equiv \rho_T \sigma_{\rm X} R_T / M_{\rm X}$, which gives a measure of the ability of the target to capture a Macro. Equation (3.44) is soluble in both the elastic and inelastic cases, however it suffices to note that the solutions are identical to $\mathcal{O}(\alpha)$ and therefore, upon the Macro's exit, the final velocity is given by

$$v_f^2 = v_0^2 - \frac{D}{R_T}\left(2v_0^2 + \frac{1}{6}\left(\frac{D}{R_T}\right)^2 v_e^2\right)\alpha + \mathcal{O}(\alpha^2)\,. \tag{3.45}$$

3.3.1 Orbital Capture Requirements

Because of spherical symmetry, it should be the case that the average value, $\langle D\rangle = 4/3 R_T$, which we will simply insert everywhere D appears in (3.45). The orbital capture requirement of $v_f < v_e$ can then be written as

$$v_0^2 - \frac{8}{3}\left(v_0^2 + \frac{4}{27}v_e^2\right)\frac{\rho_T \sigma_{\rm X} R_T}{M_{\rm X}} < v_e^2 \tag{3.46}$$

from which it follows that

$$\frac{\sigma_{\rm X}}{M_{\rm X}} \gtrsim 5\times 10^{-13}\ {\rm cm}^2/{\rm g}\ \left(\frac{R_T}{R_\odot}\right)^3 \left(\frac{v_{\rm X}}{250\ {\rm km/s}}\right)^2 \tag{3.47}$$

is needed for capture[15].

We will now specialize our discussion to nuclear-dense Macros, where $\sigma_{\rm X}/M_{\rm X} = 2.4\times 10^{-10}\,(1{\rm g}/M_{\rm X})^{1/3}\ {\rm cm}^2/{\rm g}$. Equation (3.47) indicates that Macros with masses $\gtrsim 10^5$g would not typically be captured in the sun. The dark matter presumably follows a velocity distribution, however, so there will be some fraction of Macros whose $v_{\rm X}$ is less than some critical value, $\tilde{v}$, required for capture. From (3.46), we find this velocity is approximately

$$\tilde{v} \simeq 5\ {\rm km/s}\ \left(\frac{R_\odot}{R_T}\right)^{3/2}\left(\frac{10^{18}\ {\rm g}}{M_{\rm X}}\right)^{1/6} \tag{3.48}$$

We will assume that the dark matter follows a Maxwell-Boltzmann velocity distribution, i.e. the probability distribution function is

$$f(v) = \sqrt{\frac{2}{\pi}}\frac{v^2}{\sigma_v^3}e^{-\frac{1}{2}\frac{v^2}{\sigma_v^2}}\,, \tag{3.49}$$

where $\sigma_v = 1/2\sqrt{\pi/2}\langle v\rangle$ and the distribution is normalized to satisfy[16]

$$1 = \int_0^\infty dv\ f(v)\,. \tag{3.50}$$

The probability of a Macro having an asymptotic velocity less than this is

$$\begin{aligned} P(v_{\rm X} < \tilde{v}) &= \int_0^{\tilde{v}} dv_{\rm X}\ f(v_{\rm X}) \\ &\simeq \frac{32}{3\pi^2}\left(\frac{\tilde{v}}{\langle v_{\rm X}\rangle}\right)^3\,, \end{aligned} \tag{3.51}$$

where the second line applies in the limit $\tilde{v} \ll \langle v_{\rm X}\rangle$.

3.3.2 Constraints on Nuclear-Dense Objects

Solar Constraint

It is clear that nuclear-dense macros of low mass would have no trouble being captured by the sun, so we focus our attention on the high-mass regime where $\tilde{v}$ is very small compared to $\langle v_{\rm X}\rangle$. The total number of captures, $N_{\rm cap}$, is the product of the probability given in

[15] We have used the relation $v_0^2 = v_e^2 + v_{\rm X}^2$, following from energy conservation, where $v_{\rm X}$ is the asymptotic velocity of the incoming dark matter and satisfies $v_{\rm X} < v_e$ (or $v_{\rm X} \ll v_e$) in the astrophysical systems of interest here.

[16] Technically the distribution would need to be truncated at the escape velocity of the galaxy, $v_{\rm esc}$. This would affect the overall normalization, however, models indicate that $v_{\rm esc} \gtrsim 2\langle v_{\rm X}\rangle$ (see e.g. [54]), therefore extending the integral to infinity introduces an error no larger than a few percent.

(3.51) and the total number of passages through the sun in its lifetime of 5 Gyr as determined from the rate given in (1.3). The value of $N_{\rm cap}$ for the sun apparently decreases faster than $\langle v_{\rm X}\rangle^{-2}$ with increasing $\langle v_{\rm X}\rangle$; due to a large uncertainty on the correct value of $\langle v_{\rm X}\rangle$ (see e.g. [54]) we will conservatively use the rather large value of $\langle v_{\rm X}\rangle = 300$ km/s in what follows below. From (1.3) we then find

$$N_{\rm pass} \simeq 5 \times 10^5 \left(\frac{10^{18}{\rm g}}{M_{\rm X}}\right) . \tag{3.52}$$

Inserting (3.48) into (3.51), we find that

$$P(v_{\rm X} < \tilde{v}) \sim 6 \times 10^{-6} \left(\frac{10^{18}\ {\rm g}}{M_{\rm X}}\right)^{1/2} \tag{3.53}$$

and therefore

$$N_{\rm cap} \simeq 3 \left(\frac{10^{18}\ {\rm g}}{M_{\rm X}}\right)^{3/2} . \tag{3.54}$$

The fact that our sun still shines and is well described using ordinary baryonic physics indicates it has not been converted. Using its existence to make a constraint necessarily introduces an anthropic selection bias, so we can only make the following statistical statement. Assuming the conversion (or destruction, for that matter) of our sun to be a random process, its survival probability in this context is given by

$$P_{\rm survival} = e^{-N_{\rm cap}} . \tag{3.55}$$

Therefore we can, for example, rule out $M_{\rm X} \lesssim 10^{18}$g, at 95% confidence. It becomes exponentially unlikely that such converting Macros exist at lower masses. We therefore rule out converting, nuclear-type Macros with the electromagnetic properties of model I, model II for $V_0 \lesssim 1$ keV, and model III in this mass range.

Neutron Star Constraint

Here, the orbital capture requirements are easily satisfied by any nuclear-dense Macro in the mass range of interest. Therefore $N_{\rm cap}$ is determined solely by the number of passages through a typical neutron star – for this reason we again conservatively use $\langle v_{\rm X}\rangle = 300$ km/s and find

$$N_{\rm cap} \simeq 6.2 \times \left(\frac{10^{18}{\rm g}}{M_{\rm X}}\right) \left(\frac{T_{\rm NS}}{5\ {\rm Gyr}}\right) , \tag{3.56}$$

where $T_{\rm NS}$ is the age of the neutron star and we have assumed that the dark matter density around it to be comparable to that of our local galactic neighborhood. The use of neutron stars to make a constraint on converting dark matter offers its own difficulty as it requires clear observational differences between an ordinary neutron star and whatever the converted object would be, e.g. a star that is composed, at least in part, of strange nuclear matter. For example, a pulsar's composition affects its seismology [55]; this in turn affects

its spin-down rate through an alteration in its gravitational wave emission, and this has the potential for observation through pulsar timing [56].

The crust of a neutron star, which also plays a vital role in the modeling of pulsar glitches, would determine the nature of the Macro capture. It is thought to be a dense material consisting of positively-charged nuclei, with a column density of perhaps $4 \times 10^{15}\mathrm{g/cm}^2$; this implies that nuclear-dense Macros with masses less than $\sim 10^{18}\mathrm{g}$ might only get captured in the crust, unable to penetrate to the deeper neutron-abundant regions [57]. It therefore appears that the constraints possible from neutron stars are only complementary to those from stellar objects.

4 Fruitless Ideas

Macro Luminosity: Because of the mass and size of the range of Macro parameters, they are not expected to significantly heat up material or be heated by collisions with baryonic matter in the galaxy. Regardless of their formation mechanism, we expect that they have become (and will remain) cold, and therefore dark in typical astrophysical systems. To justify this claim, we approximate the luminosity of a Macro at temperature T_{X}, to be given the Stefan-Boltzmann relation

$$\mathcal{L}_X = \frac{\pi^3}{15} R_{\mathrm{X}}^2 T_{\mathrm{X}}^4 \,. \tag{4.1}$$

At best, the Macro could hold a constant temperature by maintaining a balance between energy absorption and radiation. The rate at which energy is acquired from a surrounding gaseous environment is, at most, given by[17]

$$\pi R_{\mathrm{X}}^2 n_{gas} T_{gas} v_{\mathrm{X}} \tag{4.2}$$

and therefore, by equating (4.1) with (4.2), the Macro temperature is expected to be

$$T_{\mathrm{X}} \lesssim \sqrt[4]{\frac{15}{\pi^2} n_{gas} T_{gas} v_{\mathrm{X}}} \,, \tag{4.3}$$

which is independent of the size of the Macro, so long as it is macroscopically large. With $v_{\mathrm{X}} \approx 10^{-3} c$, we consider a few different systems: for molecular clouds in the interstellar medium, $n_{gas} \approx 10^6/\mathrm{cm}^3$ and $T_{gas} \approx 10\,\mathrm{K}$ indicating $T_{\mathrm{X}} \approx 5\,\mathrm{K}$; in the warm ionized medium $n_{gas} \approx 1/\mathrm{cm}^3$ and $T_{gas} \approx 8000\,\mathrm{K}$, resulting in $T_{\mathrm{X}} \approx 1\,\mathrm{K}$; the intracluster medium can have gas temperatures as high as $T_{gas} \approx 10^8\,\mathrm{K}$, but $n_{gas} \approx 10^{-3}/\mathrm{cm}^3$ so $T_{\mathrm{X}} \approx 2\,\mathrm{K}$. Presumably, the Macro temperature would not drop below the CMB temperature of $2.7\,\mathrm{K}$, however.

Early universe neutrinos: Compared to the canonical cosmological model where less than 20% of the matter is baryonic, the actual total number of baryons could be perhaps a

[17] The relevant velocity at which energetic particles impact the Macro is v_{X}, not the much smaller gas velocity.

factor of 6 larger if we live in a universe where the dark matter consists of Macros made of quarks. Of course, this depends on the model and how $M_{\rm X}$ scales with the baryon number, $B_{\rm X}$; for example, $M_{\rm X} \propto B_{\rm X}^{8/9}$ in Ref. [13]. A consequence of this is that, assuming that the total baryon-minus-lepton number $(B-L)$ remains fixed, the total lepton number would be commensurately larger than in the canonical case. However, since the neutrino density is almost entirely determined by thermal considerations and is already on the order of 10^9 larger than the baryon density, this appears to be a negligible effect. The neutrino mean free path would be also affected at the $\mathcal{O}(1-10)$ level[18], however, this isn't obviously observable as the neutrino thermal history remains unchanged.

CMB Opacity: One might wonder if the CMB opacity would be affected by a difference in the electron number density, Δn_e, that results from the presence of positively charged baryonic Macros. The change in electron number density depends on the Macro charge, scaling as $\Delta n_e \sim Q_{\rm X}/B_{\rm X}$ if $M_{\rm X} \propto B_{\rm X}$. In any reasonable model, if $Q_{\rm X}$ scales with $B_{\rm X}$ it will do so as $B_{\rm X}^p$, with $p \leq 2/3$ for energetic reasons. Since terrestrial constraints indicate $M_{\rm X} \gtrsim 1$ g, or $B_{\rm X} \gtrsim 10^{24}$, this strongly suggests that Δn_e would be negligible.

5 Conclusions

The nature of dark matter is still largely unknown. For this reason, it is prudent to hedge our bets on what it might be, keeping an open mind and focusing on what the observational constraints actually are – in particular for objects that interact strongly with themselves and ordinary matter, and could plausibly be accounted for within the Standard Model. Here, we have considered the class of strongly interacting dark matter, which we call *Macros*, that would have macroscopic size and mass. We have illuminated the constraints on regions of the geometric cross section vs. mass parameter space $(\sigma_{\rm X} - M_{\rm X})$ between about $10^{-15} - 10^{33}$ cm^2 and $10^{-12} - 10^{34}$ g. Ancient mica samples, the CMB and large-scale structure, as well as various gravitational lensing observations constrain only a portion of the above-mentioned parameter space. Likewise, the reduced cross section $(\sigma_{\rm X}/M_{\rm X})$ can be constrained as a function of Macro surface potential in a certain class of models wherein Macros are capable of removing baryons from the standard primordial nucleosynthesis process. Rather large regions of parameter space remain unconstrained, notably for nuclear-dense Macros of masses between $10^2 - 10^{17}$ g and $10^{20} - 10^{24}$ g.

It is conceivable that other observations not considered here can be used to make marginal improvements on the Macro constraints at low mass. Beyond the mica limits ($M_{\rm X} \gtrsim 10^2$ g), however, the Macro flux would drop below 10^{-2} km^{-2}yr^{-1} and earth-based observations are evermore limited. It is also of note that, in the unconstrained range of Macros masses between $10^2 - 10^{17}$ g, there would be between 0.1 and 10^{14} Macros occupying the sphere enclosed by the earth's orbital radius at any given time. It might be possible in the future to probe this region through local observations in our solar neighborhood. It may also be significant that, in this scenario of high-massed constituents, the dark matter's

[18] The Macros would not volume shield in the mass range of interest if they were nuclear-dense objects made of quarks.

approximation as a fluid breaks down at much larger scales than in the standard WIMP scenario. This and the possibility for dark matter to interact strongly with baryons may have interesting (and observable) astrophysical consequences.

As this manuscript was being prepared the preprint by Burdin et al. [58] came to our attention.

The authors thank Bryan Lynn for encouragement to think about standard model dark matter, and for useful conversations. We also thank Claudia de Rham, Andrew Tolley, Craig Copi, Tom Shutt, Dan Akerib, Adam Christopherson, Donnino Anderhalden, Dan Snowden-Ifft, and Amanda Weltman for discussions. During this work both authors were supported by Department of Energy grant DOE-SC0009946. One of the authors (DMJ) would also like to acknowledge support from the Claude Leon Foundation. Both authors thank the CERN Theory group for their hospitality and support during the initial phases of this work.

References

[1] S. S. McGaugh, *The halo by halo missing baryon problem*, arXiv:0707.3795.

[2] **Planck Collaboration** Collaboration, P. Ade et al., *Planck 2013 results. XVI. Cosmological parameters*, arXiv:1303.5076.

[3] **The ATLAS collaboration** Collaboration, A. Robichaud-Vronneau, *Searches for Supersymmetry and Exotics phenomena with the ATLAS detector*, *J.Phys.Conf.Ser.* **455** (2013) 012012.

[4] **CMS** Collaboration, A. Tapper, *Searches for supersymmetry with the CMS detector at the LHC*, *AIP Conf.Proc.* **1560** (2013) 59–63.

[5] **LUX Collaboration** Collaboration, D. Akerib et al., *First results from the LUX dark matter experiment at the Sanford Underground Research Facility*, *Phys.Rev.Lett.* **112** (2014) 091303, [arXiv:1310.8214].

[6] **XENON100 Collaboration** Collaboration, E. Aprile et al., *Dark Matter Results from 225 Live Days of XENON100 Data*, *Phys.Rev.Lett.* **109** (2012) 181301, [arXiv:1207.5988].

[7] **CDMS Collaboration** Collaboration, R. Agnese et al., *Silicon Detector Dark Matter Results from the Final Exposure of CDMS II*, *Phys.Rev.Lett.* **111** (2013) 251301, [arXiv:1304.4279].

[8] **Particle Data Group** Collaboration, J. Beringer et al., *Review of Particle Physics (RPP)*, *Phys.Rev.* **D86** (2012) 010001.

[9] E. Witten, *Cosmic Separation of Phases*, *Phys.Rev.* **D30** (1984) 272–285.

[10] A. De Rujula and S. Glashow, *Nuclearites: A Novel Form of Cosmic Radiation*, *Nature* **312** (1984) 734–737.

[11] E. Farhi and R. Jaffe, *Strange Matter*, *Phys.Rev.* **D30** (1984) 2379.

[12] B. W. Lynn, A. E. Nelson, and N. Tetradis, *STRANGE BARYON MATTER*, *Nucl.Phys.* **B345** (1990) 186–209.

[13] A. R. Zhitnitsky, *Dark matter as dense color superconductor*, *Nucl.Phys.Proc.Suppl.* **124** (2003) 99–102, [astro-ph/0204218].

[14] A. R. Zhitnitsky, *'Nonbaryonic' dark matter as baryonic color superconductor*, *JCAP* **0310** (2003) 010, [hep-ph/0202161].

[15] A. Zhitnitsky, *Cold dark matter as compact composite objects*, *Phys.Rev.* **D74** (2006) 043515, [astro-ph/0603064].

[16] L. Labun, J. Birrell, and J. Rafelski, *Compact Ultra Dense Matter Impactors*, *Phys. Rev. Lett. 110,* **111102** (2013) [arXiv:1104.4572].

[17] B. W. Lynn, *Liquid Phases in SU(3) Chiral Perturbation Theory (SU(3) ChPT: Drops of Strange Chiral Nucleon Liquid (S Ch NL) and Ordinary Chiral Heavy Nuclear Liquid (Ch NL)*, arXiv:1005.2124.

[18] B. J. Carr and S. Hawking, *Black holes in the early Universe*, *Mon.Not.Roy.Astron.Soc.* **168** (1974) 399–415.

[19] A. Kusenko and M. E. Shaposhnikov, *Supersymmetric Q balls as dark matter*, *Phys.Lett.* **B418** (1998) 46–54, [hep-ph/9709492].

[20] G. D. Mack, J. F. Beacom, and G. Bertone, *Towards Closing the Window on Strongly Interacting Dark Matter: Far-Reaching Constraints from Earth's Heat Flow*, *Phys.Rev.* **D76** (2007) 043523, [arXiv:0705.4298].

[21] E. Shirk and P. Price, *Charge and energy spectra of cosmic rays with z greater than or approximately equal to 60-the skylab experiment*, *The Astrophysical Journal* **220** (1978) 719–733.

[22] G. D. Starkman, A. Gould, R. Esmailzadeh, and S. Dimopoulos, *Opening the Window on Strongly Interacting Dark Matter*, *Phys.Rev.* **D41** (1990) 3594.

[23] A. Loeb and M. Zaldarriaga, *The Small-scale power spectrum of cold dark matter*, *Phys.Rev.* **D71** (2005) 103520, [astro-ph/0504112].

[24] X.-l. Chen, S. Hannestad, and R. J. Scherrer, *Cosmic microwave background and large scale structure limits on the interaction between dark matter and baryons*, *Phys.Rev.* **D65** (2002) 123515, [astro-ph/0202496].

[25] C. Dvorkin, K. Blum, and M. Kamionkowski, *Constraining Dark Matter-Baryon Scattering with Linear Cosmology*, *Phys.Rev.* **D89** (2014) 023519, [arXiv:1311.2937].

[26] L. Chuzhoy and A. Nusser, *A Limit on the dark matter and baryons interaction cross-section in galaxy clusters*, *Astrophys.J.* **645** (2006) 950–954, [astro-ph/0408184].

[27] D. N. Spergel and P. J. Steinhardt, *Observational evidence for selfinteracting cold dark matter*, *Phys.Rev.Lett.* **84** (2000) 3760–3763, [astro-ph/9909386].

[28] S. W. Randall, M. Markevitch, D. Clowe, A. H. Gonzalez, and M. Bradac, *Constraints on the Self-Interaction Cross-Section of Dark Matter from Numerical Simulations of the Merging Galaxy Cluster 1E 0657-56*, *Astrophys.J.* **679** (2008) 1173–1180, [arXiv:0704.0261].

[29] M. Rocha, A. H. Peter, J. S. Bullock, M. Kaplinghat, S. Garrison-Kimmel, et al., *Cosmological Simulations with Self-Interacting Dark Matter I: Constant Density Cores and Substructure*, *Mon.Not.Roy.Astron.Soc.* **430** (2013) 81–104, [arXiv:1208.3025].

[30] P. Price, S.-l. Guo, S. Ahlen, and R. Fleischer, *Search for GUT Magnetic Monopoles at a Flux Level Below the Parker Limit*, *Phys.Rev.Lett.* **52** (1984) 1265.

[31] P. Price and M. Salamon, *Search for Supermassive Magnetic Monopoles Using Mica Crystals*, *Phys.Rev.Lett.* **56** (1986) 1226–1229.

[32] R. Fleischer, *Tracks to innovation: Nuclear tracks in science and technology*, .

[33] P. Price, *Limits on Contribution of Cosmic Nuclearites to Galactic Dark Matter*, *Phys.Rev.* **D38** (1988) 3813–3814.

[34] A. Gould, *Femtolensing of gamma-ray bursters*, *The Astrophysical Journal* **386** (1992) L5–L7.

[35] B. Paczynski, *Gravitational microlensing by the galactic halo*, *Astrophys.J.* **304** (1986) 1–5.

[36] A. Barnacka, J. Glicenstein, and R. Moderski, *New constraints on primordial black holes abundance from femtolensing of gamma-ray bursts*, *Phys.Rev.* **D86** (2012) 043001, [arXiv:1204.2056].

[37] M. Fukugita, T. Futamase, M. Kasai, and E. Turner, *Statistical properties of gravitational lenses with a nonzero cosmological constant*, *The Astrophysical Journal* **393** (1992) 3–21.

[38] G. Marani, R. Nemiroff, J. Norris, K. Hurley, and J. Bonnell, *Gravitationally lensed gamma-ray bursts as probes of dark compact objects*, astro-ph/9810391.

[39] P. Pani and A. Loeb, *Exclusion of the remaining mass window for primordial black holes as the dominant constituent of dark matter*, arXiv:1401.3025.

[40] **EROS-2 Collaboration** Collaboration, P. Tisserand et al., *Limits on the Macho Content of the Galactic Halo from the EROS-2 Survey of the Magellanic Clouds*, *Astron.Astrophys.* **469** (2007) 387–404, [astro-ph/0607207].

[41] **(Macho Collaboration) C Alcock** Collaboration, R. Allsman et al., *MACHO project limits on black hole dark matter in the 1-30 solar mass range*, astro-ph/0011506.

[42] B. Carr, K. Kohri, Y. Sendouda, and J. Yokoyama, *New cosmological constraints on primordial black holes*, *Phys.Rev.* **D81** (2010) 104019, [arXiv:0912.5297].

[43] K. Griest, A. M. Cieplak, and M. J. Lehner, *Experimental Limits on Primordial Black Hole Dark Matter from the First Two Years of Kepler Data*, arXiv:1307.5798.

[44] C. Alcock, E. Farhi, and A. Olinto, *Strange stars*, *Astrophys.J.* **310** (1986) 261–272.

[45] A. Zhitnitsky, *The Width of the 511-KeV Line from the Bulge of the Galaxy*, *Phys.Rev.* **D76** (2007) 103518, [astro-ph/0607361].

[46] D. T. Cumberbatch, J. Silk, and G. D. Starkman, *Difficulties for Compact Composite Object Dark Matter*, *Phys.Rev.* **D77** (2008) 063522, [astro-ph/0606429].

[47] A. Kusenko, L. Loveridge, and M. Shaposhnikov, *Supersymmetric dark matter Q-balls and their interactions in matter*, *Phys.Rev.* **D72** (2005) 025015, [hep-ph/0405044].

[48] J. Madsen and K. Riisager, *STRANGE MATTER AND BIG BANG HELIUM SYNTHESIS*, *Phys.Lett.* **B158** (1985) 208–210.

[49] E. Aver, K. A. Olive, R. Porter, and E. D. Skillman, *The primordial helium abundance from updated emissivities*, *JCAP* **1311** (2013) 017, [arXiv:1309.0047].

[50] R. A. Alpher, J. W. Follin, and R. C. Herman, *Physical Conditions in the Initial Stages of the Expanding Universe*, *Phys.Rev.* **92** (1953) 1347–1361.

[51] D. A. Dicus, E. W. Kolb, A. Gleeson, E. Sudarshan, V. L. Teplitz, et al., *Primordial Nucleosynthesis Including Radiative, Coulomb, and Finite Temperature Corrections to Weak Rates*, *Phys.Rev.* **D26** (1982) 2694.

[52] R. Esmailzadeh, G. D. Starkman, and S. Dimopoulos, *Primordial nucleosynthesis without a computer*, *Astrophys. J.* (1990).

[53] S. Weinberg, *Gravitation and Cosmology*. Wiley, 1972.

[54] M. Fairbairn, T. Douce, and J. Swift, *Quantifying Astrophysical Uncertainties on Dark Matter Direct Detection Results*, *Astropart.Phys.* **47** (2013) 45–53, [arXiv:1206.2693].

[55] J. Madsen, *How to identify a strange star*, *Phys.Rev.Lett.* **81** (1998) 3311–3314, [astro-ph/9806032].

[56] M. G. Alford and K. Schwenzer, *What flashes of pulsars can teach us about their interior*, arXiv:1310.3524.

[57] J. Madsen, *Astrophysical Limits on the Flux of Quark Nuggets*, *Phys.Rev.Lett.* **61** (1988) 2909–2912.

[58] S. Burdin, M. Fairbairn, P. Mermod, D. Milstead, J. Pinfold, et al., *Non-collider searches for stable massive particles*, arXiv:1410.1374.